# Reduction of Respiratory Motion Artifacts in PET Imaging of Lung Cancer by Respiratory Correlated Dynamic PET: Methodology and Comparison with Respiratory Gated PET

Sadek A. Nehmeh, PhD[1]; Yusuf E. Erdi, DSc[1]; Kenneth E. Rosenzweig, MD[2]; Heiko Schoder, MD[3]; Steve M. Larson, MD[3]; Olivia D. Squire, BA[3]; and John L. Humm, PhD[1]

*[1]Department of Medical Physics, Memorial Sloan-Kettering Cancer Center, New York, New York; [2]Department of Radiation Oncology, Memorial Sloan-Kettering Cancer Center, New York, New York; and [3]Department of Radiology, Nuclear Medicine Service, Memorial Sloan-Kettering Cancer Center, New York, New York*

This study proposes a new method to reduce respiratory motion artifacts in PET images of lung cancer. The method is referred to as respiratory-correlated dynamic PET (RCDPET). RCDPET enables the acquisition of 4-dimensional PET data without the need for a respiratory tracking device. In this article, we compare this method with respiratory-gated PET (RGPET). Both methods provide the ability to correct for motion artifacts and more accurately quantitate radiotracer uptake within lung lesions. Both methods were evaluated in phantom studies and 1 patient. **Methods:** With RCDPET, data are acquired in consecutive 1-s time frames. A point source attached to a rigid foam block is set on the patient's abdomen and is extended into the camera field of view at the level of the lesion by means of a low-density rod. The position of this source is used to track respiratory motion through the consecutive dynamic frames. Image frames corresponding to a user-selected lesion position within the breathing cycle, in correlation with the point source position, are then identified after scanning. The sinograms of the selected image frames are summed and then reconstructed using iterative reconstruction with segmented attenuation correction. **Results:** The results from phantom studies with both RGPET and RCDPET were within 10% agreement, for both activity quantitation and image noise levels. In a clinical application, the quantitation of the $SUV_{max}$ and the lesion's size showed a 6% and 2% difference, respectively, between RCDPET and RGPET measurements. **Conclusion:** RCDPET can be considered as a comparable, or alternative, method to RGPET in reducing the smearing effects due to respiration and improving quantitation of PET in the thorax. One advantage of RCDPET over RGPET is the ability to retrospectively reconstruct the PET data at any phase or amplitude in the breathing cycle.

Received Feb. 19, 2003; revision accepted Jun. 13, 2003.

For correspondence or reprints contact: Sadek A. Nehmeh, PhD, Department of Medical Physics, Memorial Sloan-Kettering Cancer Center, 1275 York Ave., New York, NY 10021.

E-mail: nehmehs@mskcc.org

**Key Words:** PET; respiratory-gated PET; respiratory-correlated dynamic PET

**J Nucl Med 2003; 44:1644–1648**

Tumor and organ motion due to respiration is a major challenge in diagnostic imaging and in radiotherapy of lung cancer. Several diagnostic imaging techniques have been developed to improve the accuracy of determining 4-dimensional tumor coordinates (*x*, *y*, *z*, *t*) during the course of radiation therapy, including $^{18}$F-FDG PET studies (*1*,*2*), CT, and external-beam radiotherapy (*3*–*6*). Using CT and radiotherapy, breathing-synchronized radiotherapy has been developed, with modifications (*7*) such as deep inspiration breath-hold (*8*,*9*), audio (*4*) gating, and audio (*1*,*2*) without visual coaching. These methods both improve the reproducibility of the breathing motion and consequently increase precision in setting the trigger in (PET and CT) acquisition or external-beam delivery.

PET requires significantly longer scan times than CT (typically 25 min for a whole-body scan). Previously (*1*,*2*), we showed that respiratory gating may significantly improve the accuracy of tumor volume determination and of $^{18}$F-FDG quantitation in the thorax. In this study, we propose a new technique to acquire the 4-dimensional PET data, using respiratory-correlated dynamic PET (RCDPET). The main advantage of RCDPET over respiratory-gated PET (RGPET) is that it does not require a respiratory motion detector, allowing respiratory motion correction to be performed at institutions incapable of buying or developing such detectors. Moreover, RCDPET allows reconstruction of PET images at any breathing phase, retrospectively, permitting exclusion of data from irregular breathing cycles. However, image processing is more time consuming

for RCDPET than for RGPET and requires a system with more memory.

This method has been validated in phantom studies and compared with the results of RGPET, previously described (*1*,*2*). As a proof of principle, RCDPET has been clinically evaluated in a single lung cancer patient.

## MATERIALS AND METHODS

### PET/CT Scanner

Data referenced in this study were acquired on the Discovery LS PET (Advance NXi)/CT(LightSpeed 4-slice) scanner (General Electric Medical Systems). The LightSpeed CT scanner has a 50-cm transaxial field of view (FOV) and can acquire images with slice thicknesses ranging from 1.25 to 10.0 mm. Tube current can be varied between 10 and 440 mA, and tube voltage settings are 80, 100, 120, and 140 kVp. The table feed rate of the CT scanner ranges from 1.25 to 30 mm per 360° rotation of the x-ray tube. Maximum scan time per spiral is 120 s, with a spatial resolution of 0.32 mm.

The Advance PET scanner is a whole-body scanner with a transaxial field of view of 55 cm and an axial field of view of 14.75 cm. The scanner contains retractable septa and can be used in 2-dimensional mode (septa extended) or 3-dimensional mode (septa retracted) for higher sensitivity (0.032 kcps/Bq/cm$^3$). The image resolution is 4.2 mm in full width at half maximum (FWHM). All results presented here are for scanning performed in 2-dimensional mode.

### Respiratory Motion Tracking for RCDPET

In RCDPET, respiratory motion is tracked by an $^{18}$F-FDG point source attached to one end of a low-density plastic rod, and the other end of the rod is rigidly attached to a Styrofoam (The Dow Chemical Co.) block. The block is secured to the abdomen of the patient. As the patient breathes, the rod oscillates according to the respiratory motion. The length of the rod extends the point source into the FOV of the camera (Fig. 1), at a level corresponding to the approximate position of the lesion. Consequently, the point source tracing within consecutive PET frames correlates with the patient's breathing motion.

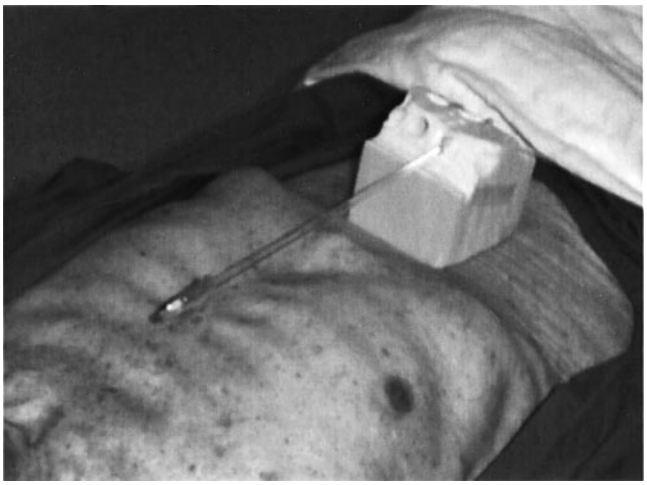

**FIGURE 1.** Patient setup in RCDPET acquisition mode. Point source is at end of low-density rod, extending into lesion FOV, and rigidly attached to Styrofoam (The Dow Chemical Co.) block positioned on abdomen of patient.

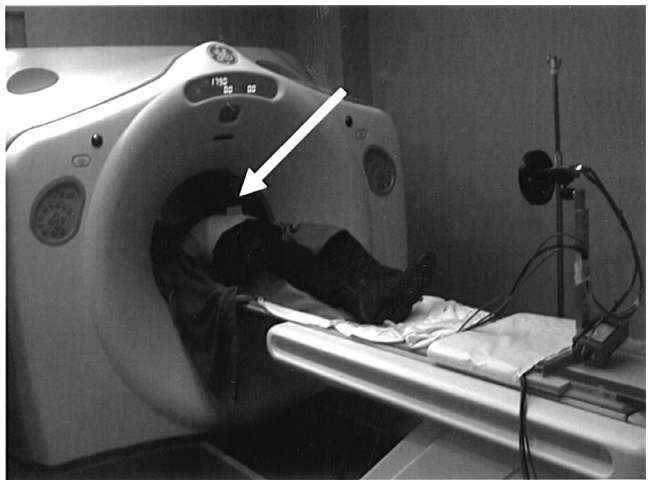

**FIGURE 2.** Patient setup in RGPET acquisition mode. Plastic block (arrow) with 2 infrared passive reflectors is positioned on abdomen of patient. Infrared camera, positioned on PET table, is used to trace motion of reflectors and, thus, patient breathing motion.

### Respiratory Motion Tracking for RGPET

For RGPET, the Real-Time Position Management (RPM) Respiratory Gating system (Varian Medical Systems) was used. This device was initially designed for radiotherapy gating. The RPM system monitors the motion of the chest wall of the patient (thus the respiratory motion) by tracking the vertical position of 2 passive reflective markers rigidly mounted on a lightweight plastic block. The block is stabilized on the patient's abdomen, and its motion is monitored and tracked using an infrared video camera mounted on the PET table (Fig. 2). The motion of the block is displayed by a graphic interface on the screen of the RPM workstation.

A training session was performed before the scan to obtain a prototype of the breathing motion as defined by the RPM system and to determine whether the patient breathing cycle was regular. The RPM system generates a trigger signal at a user-selected phase or amplitude within the breathing cycle. A trigger is generated by the RPM system every time the phase (amplitude) of the breathing cycle is regular at the defined position, compared with the prototype. More details about the RPM system can be found in Kubo et al. (*4*).

### Data Acquisition and Processing

A CT scan was first acquired at 140 keV and used for attenuation correction of the PET emission images. The 140-keV CT data were then transformed to the corresponding values at 511-keV energy and were reconstructed into CT attenuation correction maps, using the software provided with the PET/CT scanner.

RCDPET data were acquired into 1-s (maximum temporal resolution of PET) consecutive frames using the standard dynamic scanning mode provided by the PET scanner software. Two hundred 1-s frames were acquired. RCDPET studies did not require any additional computer hardware. However, they required ~200 times more memory per field of view than a standard emission scan (~229 MB vs. ~1.14 MB).

All 200 frames were reconstructed using an algorithm: iterative reconstruction with segmented attenuation correction (IRSAC). A square region of interest (ROI) was drawn and positioned over the image of the point source, at a user-selected position within the breathing cycle. In the phantom study, the simulated lesion was contoured instead. The ROI was then copied over all 200 frames. The frames in which the point source fell within the ROI were then identified. The sinograms corresponding to the identified time frames were added and then reconstructed using the IRSAC algorithm.

In the gated acquisition mode, each oscillatory cycle was divided into five 1-s bins, defined to encompass the respiratory cycle. The RPM system was used to initiate the trigger at a defined phase or amplitude during the oscillatory motion, as described in Nehmeh et al. (*1*,*2*). The output was 5 images, each corresponding to 1 position of the lesion within the oscillatory motion.

For all PET studies, the data were reconstructed into 128 × 128 matrices using the IRSAC algorithm and then corrected for attenuation (using the CT attenuation correction data), scatter, and randoms using the manufacturer-supplied software.

### Phantoms

Phantom measurements were performed using a $^{68}$Ge rod source (4.7-mm outer diameter) with an activity of 9.25 MBq distributed over a length of 14.5 cm. This rod source was attached to a breathing phantom (Varian Medical Systems) to simulate human respiratory motion. The $^{68}$Ge rod source was pivoted at one end, and the other end oscillated in the vertical plane along the PET gantry axis (Fig. 3). The maximum amplitude was approximately 4.0 cm in the vertical plane, with a period of 5 s.

Thirty-five transaxial PET images, each corresponding to 1 oscillation amplitude, were reconstructed along the $^{68}$Ge rod source. A 3-min nongated emission scan (static), a 5-min gated emission scan (5 bins, 1 s each), and a 200-s dynamic scan (200 frames, 1 s each) were acquired. The period of the oscillatory motion of the breathing phantom was adjusted to about 5 s, comparable to a typical patient respiratory cycle.

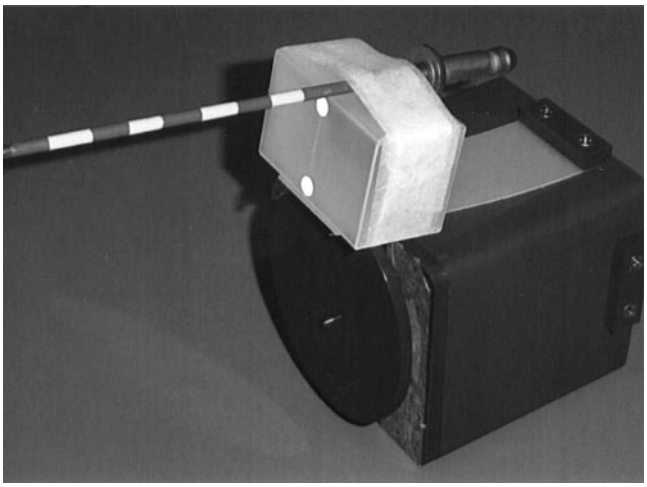

**FIGURE 3.** $^{68}$Ge rod source is mounted to Varian breathing phantom, pivoted at phantom side, and other end is free to oscillate vertically. Rod source has activity of 9.25 MBq and outer diameter of 4.7 mm.

### Patient Data

We evaluated the RCDPET technique and compared it with RGPET in 1 male patient with non–small cell lung cancer. The patient had already undergone CT simulation for radiation treatment planning on an AcQSim (Picker International). He was positioned supine with the arms up, using a mold (Alpha Cradle Molds) to assist immobilization.

During the PET session, the patient was instructed to breathe regularly for 5 s by following audio breathing instructions originally generated and adapted to his breathing motion during the simulation session. The audio coaching was created by Cool Edit 2000 software (Adobe Systems Inc.). The patient was then injected intravenously with 0.45 MBq of $^{18}$F-FDG. This was followed by an uptake phase with the patient recumbent for 45 min. The patient was then repositioned as during radiotherapy simulation, underwent a scout scan on the CT scanner, and then underwent a helical CT scan, which was used for attenuation correction and anatomic localization of the PET images. A static (nongated) whole-body 2-dimensional emission PET scan was then acquired for clinical management and treatment planning. The standard lung PET protocol at our center consists of 5 fields of view (14.25 cm per field of view). The total scan time is 20 min, with 4 min per FOV. An RGPET study was then performed for just 1 bed position (at the lesion site), using the RPM system to track the motion of the gating block on the chest of the patient. This study consisted of a 5-min gated emission scan, with 1 min per bin (i.e., 5 bins). This scan was followed by a 200-s RCDPET study (1 s/frame), during which a point source of ~9.25 MBq was placed within the field of view to track the diaphragm motion. The patient was continually coached during both RGPET and RCDPET to minimize any irregularity in the breathing cycle.

### Analysis

In the static acquisition (both nonoscillating and oscillating states), the lesion was contoured after setting the lower threshold to 42% of the maximum activity concentration ($Act\_Conc_{max}$) within the lesion, as recommended by Erdi et al. (*10*). This contouring was done on an image-by-image basis. The $Act\_Conc_{max}$ within each ROI was measured. Because, in the phantom study, the radioactive rod was pivoted at one end, each transaxial image corresponded to a different amplitude.

In the RCDPET study, all frames that corresponded to a user-selected lesion position were identified, and their corresponding sinograms were summed. Each set of summed sinograms was then reconstructed. The lesion was contoured, and then the $Act\_Conc_{max}$ within each ROI in all transaxial slices containing the lesion was recorded.

In the gated study, the images that corresponded to the most highly synchronized bin (first bin) (*1*,*2*) were analyzed. Again, the lesion was contoured, and then the $Act\_Conc_{max}$ was determined in all the transaxial slices.

To compare the relative efficiency of the RCDPET and RGPET methods in recovering the correct activity concentration in the rod or lesion, the percentage difference in $Act\_Conc_{max}$ was defined as:

$$\%Difference = abs\left[\frac{(Act\_Conc\max|_{RCDPET} - Act\_Conc\max)|_{RGPET})}{(Act\_Conc\max|_{RCDPET} + Act\_Conc\max|_{RGPET})/2}\right] \times 100. \quad \text{Eq. 1}$$

This percentage difference was calculated on a slice-by-slice basis.

For the phantom study, the SD ($\sigma$) of the activity concentration within the source was analyzed to compare the relative noise of the

2 methods. The comparative noise level was evaluated by the percentage difference in the SD between the 2 methods, given by:

$$\%Difference = abs\left[\frac{(\sigma|_{RCDPET} - \sigma|_{RGPET})}{(\sigma|_{RCDPET} + \sigma|_{RGPET})/2}\right] \times 100. \quad \text{Eq. 2}$$

## RESULTS

The measured Act_Conc$_{max}$ for an oscillating rod source is plotted in Figure 4A as a function of the amplitude for 3 acquisition modes: static, gated (RGPET), and dynamic (RCDPET). Figure 4A also shows the Act_Conc$_{max}$ for the stationary source, which is considered the reference standard. With the RCDPET technique, the correct Act_Conc$_{max}$, and consequently the standardized uptake value (SUV), could be recovered. In our previous publications (*1*,*2*), we proved that the FWHM of the activity concentration distribution within a lesion (lesion size) and the Act_Conc$_{max}$ are correlated. Thus, a change in the apparent lesion size due to motion blurring will result in, ideally, an equivalent change in the Act_Conc$_{max}$. Consequently, a correction in the Act_Conc$_{max}$ will allow recovery of the stationary lesion size. The percentage difference in the Act_Conc$_{max}$ for different motion amplitudes between the 2 techniques shows an agreement within 10%. An evaluation of the noise level within the source for the different motion amplitudes is shown in Figure 4B. This figure shows comparable noise levels (within 10%) by both approaches, demonstrating that there are no significant statistical noise penalties to respiratory phase rebinned dynamic scans.

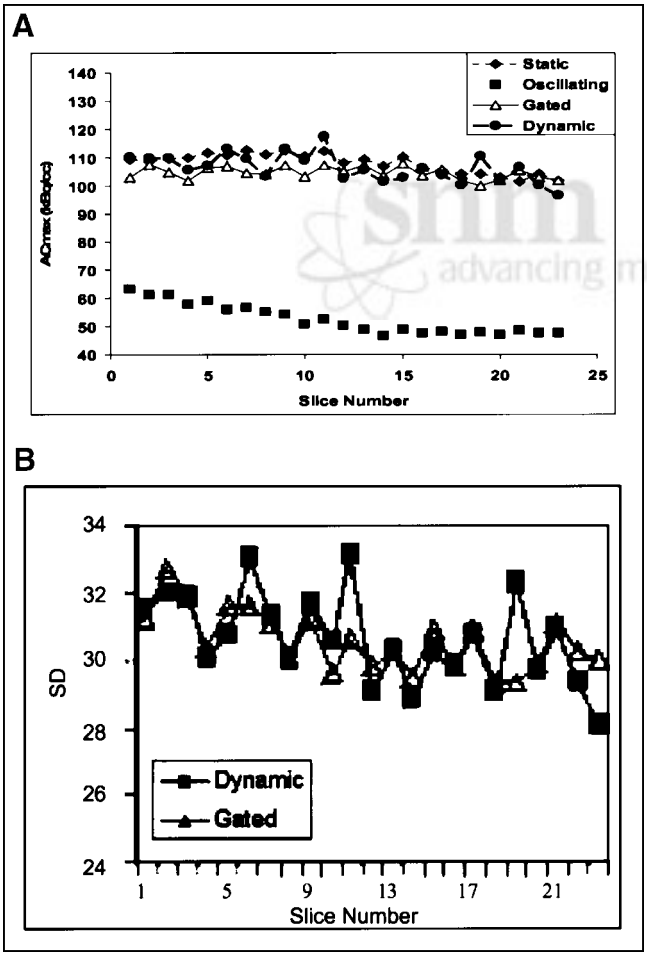


**FIGURE 4.** (A) Act_Conc$_{max}$ versus slice number (amplitude). RCDPET technique shows capability comparable to that of RGPET technique in recovering correct Act_Conc$_{max}$, which is distorted because of respiratory motion. (B) SD of activity concentration within multiple transaxial slices of lesion (thus motion amplitudes), measured in both RCDPET and RGPET techniques, shows comparable noise level. AC$_{max}$ = Act_Conc$_{max}$.

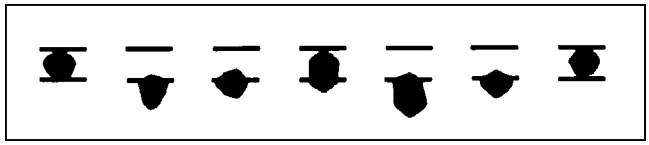

**FIGURE 5.** Position of point source as it moves in and out of user-selected reference position (e.g., as defined by the 2 lines according to position of point source in first frame) in consecutive 1-s time frames. Position of point source defines fourth dimension (time) of lesion coordinates.

In the clinical evaluation, the placement of the $^{18}$F-FDG point source with ~9.25 MBq of activity did not show any pronounced streak artifacts in the patient emission images. The point source position (which reflects the breathing motion) through consecutive time frames is illustrated in Figures 5 and 6, which show transaxial views of the lesion in RGPET and RCDPET, respectively. The maximum SUV and the lesion size in the corresponding slice were 3.56 g/mL and 2.54 cm$^2$, respectively, as measured with RGPET. The corresponding RCDPET measurements were within a 6% and a 2% difference from the RGPET measurements. The amplitude of the lesion motion by both methods was consistent within the PET axial spatial resolution (4.25 mm).

## DISCUSSION

We have shown that RCDPET corrects for the motion artifacts caused by respiration during PET imaging of lung cancer. This was shown in phantom studies, and feasibility was demonstrated in a single patient. Even though we intend to use this technique in $^{18}$F-FDG PET imaging, the approach is applicable to any PET tracer. Phantom studies showed that RCDPET improves the accuracy of quantitating within-lesion activity, which can be seriously underestimated because of respiratory motion. This rearrangement of the counts within the apparent lesion volume is also accompanied by images that more accurately reflect the lesion size and shape, as we have shown in our previous studies (*1*,*2*).

The RCDPET method yields comparable results to the respiratory gating technique in the ability to correct for the activity concentration distribution within the lesion, SUV, lesion size, and lesion shape. Phantom studies using both techniques also show a comparable noise level, independent of the smearing amplitude.

The major advantages of RCDPET are, first, that it does not require any additional tracking hardware to monitor and

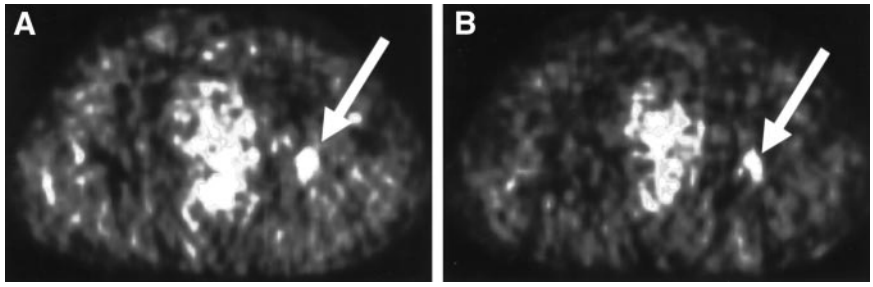


**FIGURE 6.** Transaxial view of lesion (arrow) in RGPET (A) and RCDPET (B).

trace respiratory motion. This may be a major benefit for small institutions that do not have a gating system. A second advantage is that no significant effort is required from the patient, such as is the case when a spirometer is used. Third, data selection is performed retrospectively, as compared with before scanning in RGPET, which requires the selection of a trigger position a priori. An additional advantage is that the method is less susceptible to irregular breathing and allows the user to drop irregular data from the reconstructed images. Finally, the data can retrospectively be reconstructed for any breathing phase or amplitude. This ability allows PET data to be selected to exactly match the phase of the CT image data acquired on a PET/CT unit and during radiotherapy CT simulation.

On the other hand, RCDPET requires significantly more computer memory, postprocessing time, and image reconstruction time than does RGPET. Another disadvantage of RCDPET versus RGPET is that the time resolution (defined by the PET software) is 1 s, compared with 0.013 s in the PET gated acquisition mode.

The RCDPET method can allow more accurate matching between the CT images (obtained during simulation for radiotherapy patients) and the PET images, which may be a great benefit both for PET/CT diagnostic scanning and for PET/CT planned respiratory-gated radiotherapy. In both instances, the respiratory phases can be matched between PET and CT. This method has already been developed at our institution to correlate CT slices with time. This correlation, when associated with the RCDPET method, may then allow after-scanning selection of the PET/CT phase at which radiotherapy may be planned.

## CONCLUSION

In our study we have shown the feasibility of using RCDPET, as an alternative method to RGPET, to correct for respiratory motion artifacts in PET images. RCDPET was compared with RGPET in phantom studies and was evaluated in a single patient. Like RGPET, RCDPET enabled recovery of the static SUV and determined the tumor burden. The main advantage of this new technique over RGPET is that it does not require additional instrumentation. However, RCDPET does involve a greater computational overhead associated with retrospective image data analysis.

## ACKNOWLEDGMENTS

The authors thank all those who have contributed to these promising results, in particular Dr. Hassan Mostafavi from Varian, for his help in providing the proper phantom to perform this experiment, and Steve Kohlmyer from General Electric Medical Systems, for helpful information about dynamic PET acquisition.

## REFERENCES

1. Nehmeh SA, Erdi YE, Ling CC, et al. Effect of respiratory gating on reducing lung motion artifacts in PET imaging of lung cancer. *Med Phys.* 2002;29:366–371.
2. Nehmeh SA, Erdi YE, Ling CC, et al. Effect of respiratory gating on quantifying positron emission tomography images of lung cancer. *J Nucl Med.* 2002;43:876–881.
3. Kubo HD, Hill BC. Respiration gated radiotherapy treatment: a technical study. *Phys Med Biol.* 1996;41:83–91.
4. Kubo HD, Len PM, Minohara S, Mostafavi H. Breathing-synchronized radiotherapy program at the University of California Davis Cancer Center. *Med Phys.* 2000;27:346–353.
5. Ramsey CR, Scaperoth D, Arwood D, Oliver AL. Clinical efficacy of respiratory gated conformal radiation therapy. *Med Dosim.* 1999;24:115–119.
6. Ramsey CR, Cordrey IL, Oliver AL. A comparison of beam characteristics for gated and nongated clinical x-ray beams. *Med Phys.* 1999;26:2086–2091.
7. Kubo HD, Wang L. Introduction of audio gating to further reduce organ motion in breathing synchronized radiotherapy. *Med Phys.* 2002;29:345–350.
8. Mah D, Hanley J, Rosenzweig K, et al. Technical aspects of the deep inspiration breath hold technique in the treatment of lung cancer. *Int J Radiat Oncol Biol Phys.* 2000;48:1175–1185.
9. Rosenzweig K, Hanley J, Mah D, et al. The implementation of the deep inspiration breath hold technique in the treatment of inoperable non-small cell lung cancer. *Int J Radiat Oncol Biol Phys.* 2000;48:81–87.
10. Erdi Y, Mawlawi O, Larson S, et al. Segmentation of lung lesion volume by adaptive positron emission tomography image thresholding. *Cancer.* 1997;80:2505–2509.